

Iterative Solution of Eddy Current Problems on Polyhedral Meshes

Paolo Bettini^{ID1}, Mauro Passarotto², and Ruben Specogna^{ID2}

¹Department of Industrial Engineering, University of Padova, 35131 Padua, Italy

²Polytechnic Department of Engineering and Architecture, Università di Udine, 33100 Udine, Italy

We present an effective technique to solve eddy current problems on the conductors of arbitrary topology by an iterative geometric formulation suitable for an arbitrary polyhedral mesh. The formulation is based on the reformulation of the volume integral formulation in a form suitable to be solved by fixed point iterations. Given that nowadays, the computation of Biot-Savart fields can be performed efficiently on graphics processing units, the right-hand side of the systems is constructed at each fixed point iteration without computing the inductance matrix, which is fully populated. The proposed technique is useful in eddy current problems at industrial frequency where meshing the complement of conductors is hard, thus representing a sound alternative to integral formulations.

Index Terms—Cohomology, discrete geometric approach, eddy currents, finite elements, fixed point.

I. INTRODUCTION

THIS paper addresses the solution of eddy current problems in conducting the structures of arbitrary topology by means of a geometric integral formulation suitable for a general polyhedral mesh. The formulation may be derived from the geometric integral formulation introduced in [1], which is similar to the finite element counterpart [2]. The main differences are that [1] is suitable with general polyhedral meshes and the topological pre-processing is performed much faster, thanks to state of the art algorithms as the Dłotko-Specogna (DS) [3].

Assuming, for the sake of simplicity, that the conductor is topologically trivial, either of the formulations [1] or [2] may be written as a linear system

$$(\mathbf{K}_R + i \mathbf{K}_M) \mathbf{T} = \mathbf{b}_s \quad (1)$$

where \mathbf{K}_R and \mathbf{K}_M are the real and imaginary part of the system matrix, respectively, and \mathbf{b}_s is the right-hand side (RHS). Finally, \mathbf{T} is the vector of unknowns that can be interpreted as the integral of the electric vector potential on mesh edges (or on cotree edges if the standard tree-cotree gauge [2] is applied). We remark that \mathbf{K}_M is fully populated, while \mathbf{K}_R is very sparse.

The main idea, inspired from [4] and [5], stems from rewriting the linear system as

$$\mathbf{K}_R \mathbf{T} = -i \mathbf{K}_M \mathbf{T} + \mathbf{b}_s \quad (2)$$

which yields

$$\mathbf{T} = -i \mathbf{K}_R^{-1} \mathbf{K}_M \mathbf{T} + \mathbf{K}_R^{-1} \mathbf{b}_s. \quad (3)$$

Manuscript received June 27, 2017; revised September 4, 2017; accepted October 12, 2017. Date of publication November 14, 2017; date of current version February 21, 2018. Corresponding author: P. Bettini (e-mail: paolo.bettini@unipd.it).

Color versions of one or more of the figures in this paper are available online at <http://ieeexplore.ieee.org>.

Digital Object Identifier 10.1109/TMAG.2017.2765925

Then, (3) is solved by a fixed point iteration, that is

$$\mathbf{T}^n = -i \mathbf{K}_R^{-1} \mathbf{K}_M \mathbf{T}^{n-1} + \mathbf{K}_R^{-1} \mathbf{b}_s. \quad (4)$$

We remark that, similar to the T-method [4], the matrix \mathbf{K}_M still has to be assembled. Since this matrix is full, it requires too much memory to be stored in a computer for large problems. The novelty of this contribution is twofold: how to introduce an alternative technique that avoids the computation of matrix \mathbf{K}_M and how to deal with non-simply connected conductors.

Instead of computing \mathbf{K}_M , it is in fact advantageous to compute the RHS of (3) at each fixed point step by Biot-Savart law. This can be performed very quickly nowadays by performing the computations on a graphics processing unit [6]. Applications where the proposed formulation is most useful are the ones for which the generation of the mesh in the complements of conductors may be problematic. A possible example is in nuclear fusion applications, where the complexity of the conducting structures surrounding the plasma can prevent the generation of the mesh in air, as required by standard differential formulations. For this reason, these problems are often solved by means of integral formulations. Nonetheless, a fine discretization of the conductors require the adoption of advanced techniques (e.g., fast multipole method or adaptive cross approximation coupled with hierarchical matrix arithmetics) to avoid impractical memory requirements. The proposed formulation is a simple and sound alternative.

This paper is organized as follows. Section II introduces the iterative eddy current formulation by using the geometric framework. Section III exposes the convergence criteria and issues related to the choice of a fixed point scheme. In Section IV, some results to validate the method are shown. Finally, in Section V, the conclusions are drawn.

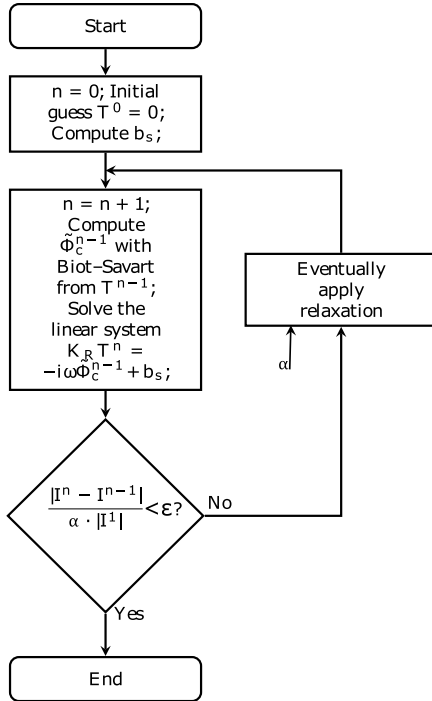


Fig. 1. Iterative solution of an eddy current problem.

II. NOVEL FORMULATION

For the formulation, we will resort to the construction of the barycentric dual complex whose details are exposed in [7]. The whole algorithm is represented in Fig. 1. Before starting the cycle, the arrays \mathbf{b}_s is computed. In our geometric formulation, this is obtained with

$$\mathbf{b}_s = -i\omega \mathbf{C}^T \tilde{\mathbf{A}}_s \quad (5)$$

where ω is the angular frequency, \mathbf{C} is the sparse matrix containing the incidences between the face and edge pairs, and $\tilde{\mathbf{A}}_s$ is the integral of the magnetic vector potential (computed by using the Biot–Savart law) on dual edges of the mesh due to the source currents only.

Then, a cycle is performed until the current update

$$\frac{|\mathbf{I}^n - \mathbf{I}^{n-1}|}{\alpha \cdot |\mathbf{I}^n|} = \frac{|\mathbf{C}^T \mathbf{T}^n - \mathbf{C}^T \mathbf{T}^{n-1}|}{\alpha \cdot |\mathbf{C}^T \mathbf{T}^n|} \quad (6)$$

is below a user-defined tolerance ε . The constant α is the relaxation parameter. In each iterate, the old current density inside mesh elements is found by multiplying the face basis functions [8] by the current vector $\mathbf{I}^{n-1} = \mathbf{C}^T \mathbf{T}^{n-1}$ on mesh faces. Then, the magnetic flux $\tilde{\Phi}_c^{n-1}$ on dual faces produced by eddy currents is computed as

$$\tilde{\Phi}_c^{n-1} = \mathbf{C}^T \tilde{\mathbf{A}} \quad (7)$$

where the magnetic vector potential integrated on dual edges $\tilde{\mathbf{A}}$ is found with Biot–Savart law from the induced current density. Finally, the new distribution of current is found by solving a sparse linear system

$$\mathbf{K}_R \mathbf{T}^n = -i\omega \tilde{\Phi}_c^{n-1} + \mathbf{b}_s \quad (8)$$

which enforces the discrete Faraday's law. We remark that the sparse matrix \mathbf{K}_R contains only real entries. Moreover, we underline that one may use any div-conforming method to compute such current. For example, we use the gauged or ungauged electric vector potential formulation.

The proposed algorithm works also for non-simply connected conductors, provided that cohomology basis functions are used inside the electric vector potential formulation.

A. Non-Simply Connected Domains

As explained in [1], when dealing with non-simply connected domains, the system to be solved becomes

$$\mathbf{K}\mathbf{T} + (\mathbf{KH})\mathbf{i} = -i\omega \mathbf{C}^T \tilde{\mathbf{A}}_s \quad (9)$$

$$(\mathbf{H}^T \mathbf{K})\mathbf{T} + (\mathbf{H}^T \mathbf{KH})\mathbf{i} = -i\omega \mathbf{H}^T \mathbf{C}^T \tilde{\mathbf{A}}_s \quad (10)$$

with $\mathbf{K} = \mathbf{K}_R + i\mathbf{K}_M$ and where the matrix \mathbf{H} stores a set of representatives of the first cohomology group generators $H^1(\partial\mathcal{K}, \mathbb{Z})$ of the boundary $\partial\mathcal{K}$ of the conductors. Moreover, the array \mathbf{i} contains the unknown independent currents due to the non-local Faraday's law.

If we now apply (8) to (9) and (10), we obtain the final iterative formulation to be used with non-simply connected conductors

$$\mathbf{K}_R \mathbf{T}^n + (\mathbf{K}_R \mathbf{H}) \mathbf{i}^n = -i\omega (\tilde{\Phi}_c^{n-1} + \mathbf{C}^T \tilde{\mathbf{A}}_s) \quad (11)$$

$$(\mathbf{H}^T \mathbf{K}_R) \mathbf{T}^n + (\mathbf{H}^T \mathbf{K}_R \mathbf{H}) \mathbf{i}^n = -i\omega \mathbf{H}^T (\tilde{\Phi}_c^{n-1} + \mathbf{C}^T \tilde{\mathbf{A}}_s). \quad (12)$$

III. CONVERGENCE CRITERIA

Method convergence is the main issue related to an iterative approach. In fact, the proposed fixed point formulation is not always convergent. In most cases, as shown in Fig. 1, the relaxation parameter α has to be applied to the system RHS in order to obtain a convergent solution. Referring, for the sake of simplicity, to the simply connected domain formulation (8) the system RHS term consequently becomes

$$\mathbf{K}_R \mathbf{T}^n = \text{RHS}^{n-1} \quad (13)$$

$$\text{RHS}^{n-1} = \alpha(-i\omega \tilde{\Phi}_c^{n-1} + \mathbf{b}_s) + (1-\alpha)(\text{RHS}^{n-2}). \quad (14)$$

According to [9, pp.99–101], given an arbitrary linear system in the classic form

$$\mathbf{Ax} = \mathbf{b} \quad (15)$$

the left-hand side of the equation can be split as

$$(\mathbf{S} + \mathbf{D})\mathbf{x} = \mathbf{b} \quad (16)$$

aiming at solving the system as the fixed point iteration

$$\mathbf{S}\mathbf{x}^n = -\mathbf{D}\mathbf{x}^{n-1} + \mathbf{b}. \quad (17)$$

After defining the so-called *iteration matrix* \mathbf{P} according to the relations

$$\mathbf{x}^n = -(\mathbf{S}^{-1}\mathbf{D})\mathbf{x}^{n-1} + \mathbf{S}^{-1}\mathbf{b} \quad (18)$$

$$\mathbf{P} = \mathbf{S}^{-1}\mathbf{D} \quad (19)$$

it has to be

$$\|\mathbf{P}\| < 1 \quad (20)$$

in order to ensure the method convergence.

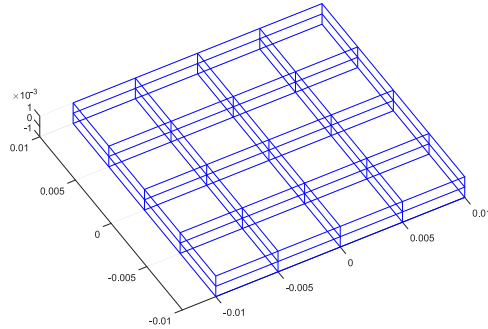


Fig. 2. Slab with coarsest discretization.

Since for the novel proposed formulation, it is not possible to rewrite the problem system (8) as in (18), we resort to [10] where, even if a slight different formulation is used, it is suggested that, in order to obtain that method convergence, it has to be

$$0 < \alpha < \frac{1}{1 + \frac{4}{3} \left(\frac{R}{\delta} \right)^4} \quad (21)$$

where R is the radius of the smallest ball containing the conducting domain and δ is the penetration depth, given the well-known relation

$$\delta = \sqrt{\frac{\rho}{\pi \mu f}} \quad (22)$$

with ρ conductors resistivity, μ magnetic permeability, and f the electromagnetic fields frequency. Consequently, this condition suggests to choose $\alpha \leq 1$ also for our formulation.

Since, as already mentioned, this novel formulation deeply differs from that one used in [10], we are interested in investigating whether the relation between α , R , and δ is the same with the currently proposed iterative scheme too.

A. Convergence Tests

Aiming at understanding the convergence behavior of this novel formulation in function of α , R , ρ , and f , several tests have been carried out using a simple geometry, inspired by [4]. A slab of dimensions 20 mm \times 20 mm \times 2 mm, shown in Fig. 2 was used, performing different discretizations with increasing grain in order to vary the volumes number (three different grids with 32, 256, and 1048 hexahedral elements were realized). For each different tests, the slab was exposed to an external magnetic induction field $B = 1$ T vertically applied.

First, the convergence velocity with varying α and frequency was investigated, setting as constant the other parameters involved. This paper has been realized for each differently grained mesh to verify that the mesh density does not affect the convergence behavior. In particular, Fig. 3 (top graph) shows that no over-relaxation ($\alpha > 1$) is effective to accelerate the convergence and so the optimal α in non-critical conditions is $\alpha = 1$; differently, the bottom graph of Fig. 3 suggests that as the frequency increases the number of required iteration increases too. It is important to notice that in this second test the presented results were obtained with $\alpha = 0.01$; this

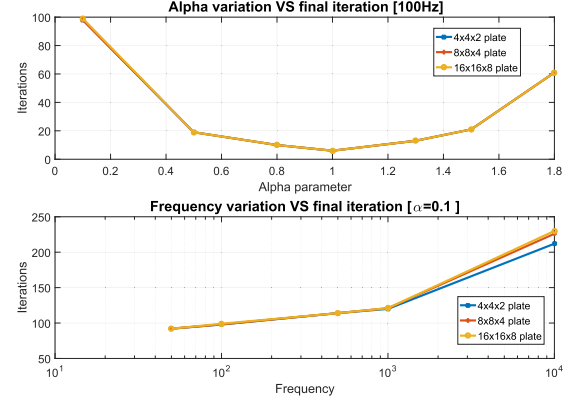


Fig. 3. Top: required iterations with relaxation parameter α and mesh grain variation. Bottom: required iterations trend with frequency and mesh grain variation.

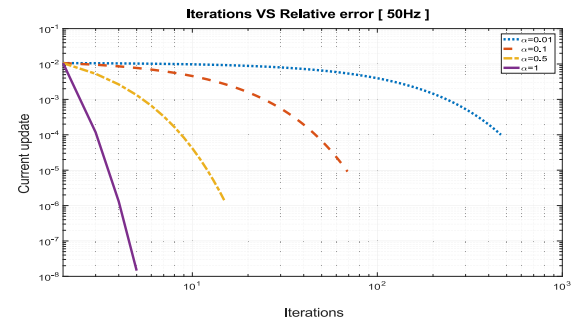


Fig. 4. Current update up to convergence trend with relaxation parameter α variation.

TABLE I
OVERALL DOMAIN SIZE VARIATION

| Domain size | 1:1 | 10:1 | 50:1 |
|----------------------|-----|------|------|
| α_{max} value | 1 | 0.5 | 0.01 |
| Iterations | 5 | 30 | 964 |

choice is due to the fact that this α value is the maximum value that guarantees the convergence for each frequency reported in the graph. With a greater α , the tests with the highest frequencies ($f = 1$ kHz and $f = 10$ kHz) would not converge. For both the mentioned graphs, all the three already presented meshes have been used and the related results have been reported: no dependence by the mesh grain has been evidenced.

In Fig. 4, the current update respect to the required number of iterations with varying α values is shown. The smaller is the relaxation parameter, the higher the iterations value. Once again, since the electromagnetic field frequency is low ($f = 50$ Hz) the best result has been obtained with $\alpha = 1$, while with the other values performances are worse. For sake of clearness, we underline that this does not mean that $\alpha = 1$ is always the best choice, in fact with *critical* conditions a smaller α is necessary. In order to better define these critical conditions another test is necessary: overall mesh size variation. This aspect is treated in Table I; the original slab dimensions were enlarged ($\times 10$ and $\times 50$) and the correspondent maximum α value to obtain a convergent solution ($\varepsilon = 10^{-6}$) was reported for each test.

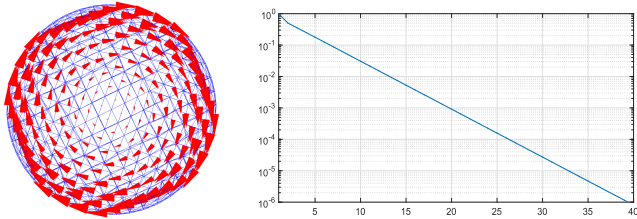


Fig. 5. Left: eddy currents induced in a solid sphere (radius $r = 50$ mm and resistivity $\rho = 0.1 \mu\Omega\text{m}$) subject to a uniform sinusoidal magnetic field ($B = 1$ T and $f = 50$ Hz) in the direction perpendicular to the page; red cones are the imaginary part of the current density. Right: convergence of the method. Current update is a function of the number of iterations n .

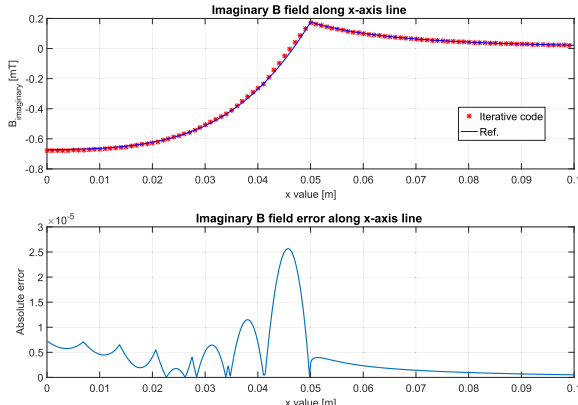


Fig. 6. Magnetic induction field due to the imaginary part of the eddy current induced in the sphere and related absolute error.

In conclusion, it is possible to state that also with the currently proposed novel iterative formulation, the behavior is qualitatively in accordance with (21): the bigger is the overall mesh size R the smaller has to be the α value, the higher is the skin depth δ the higher is the optimal α .

IV. NUMERICAL RESULTS

The proposed approach has been applied to calculate the currents induced in a solid sphere (radius $r = 50$ mm and resistivity $\rho = 0.1 \mu\Omega\text{m}$) subject to a uniform sinusoidal magnetic field ($B = 1$ T and $f = 50$ Hz). The numerical domain is covered by a polyhedral mesh consisting of 1840 elements, 7256 faces, 7326 edges, and 1911 nodes. The total number of degrees of freedoms (DoFs) is 4329. The relaxation parameter applied to ensure the solution convergence was $\alpha = 0.5$, thus the required iterations number is in good accordance with the previous convergence tests. The solution, shown in Fig. 5, is in excellent agreement with the one obtained with the volume integral formulation presented in [1]. In fact, in Fig. 6 a comparison between the solution of this iterative formulation and an analytical solution of the problem is presented. Particularly, the trend of the magnetic induction field caused by the induced currents and the related error are reported. Both graphs lead to state that the error is limited.

Finally, in Fig. 7 the solution of a non-simply connected conducting structure is presented. To perform this simulation the efficient DS algorithm [3] was implemented and applied to the novel iterative formulation. Once again results are in accordance with that one obtainable with [1]. The plate has dimensions 100 mm \times 100 mm \times 25 mm and was exposed

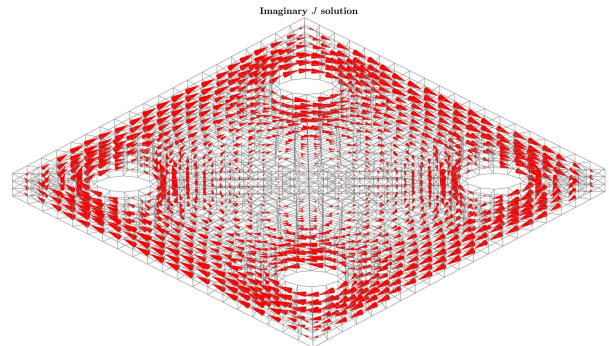


Fig. 7. Imaginary part of the eddy current induced in the conducting structure.

to a uniform vertical magnetic field $B = 1$ T. The polyhedral mesh yields to 2549 DoFs. The conductor resistivity was set to $\rho = 10 \mu\Omega\text{m}$ and the frequency $f = 50$ Hz. Convergence ($\varepsilon = 10^{-6}$) was reached in three iterations using $\alpha = 1$.

V. CONCLUSION

An iterative formulation to solve eddy current problems has been presented. Possibilities and limits of this new formulation have been shown with a particular attention for the convergence criteria in order to establish the applications boundaries.

ACKNOWLEDGMENT

This work was supported in part by the Department of Industrial Engineering, University of Padova, Padua, Italy, under Grant BIRD162948/1, and in part by the Head Higher Education and Development Operation 1 UNIUD Project, Friuli-Venezia Giulia, Italy.

REFERENCES

- [1] P. Bettini, M. Passarotto, and R. Specogna, "A volume integral formulation for solving eddy current problems on polyhedral meshes," *IEEE Trans. Magn.*, vol. 53, no. 5, Jun. 2017, Art. no. 7204904.
- [2] R. Albanese and G. Rubinacci, "Integral formulation for 3D eddy-current computation using edge elements," *IEEE Proc. A Phys. Sci., Meas. Instrum., Manage. Edu. Rev.*, vol. 135, no. 7, pp. 457–462, Sep. 1988.
- [3] P. Dłotko and R. Specogna, "Physics inspired algorithms for (co)homology computations of three-dimensional combinatorial manifolds with boundary," *Comput. Phys. Commun.*, vol. 184, no. 10, pp. 2257–2266, Oct. 2013.
- [4] T. Takagi, T. Sugiura, K. Miyata, S. Norimatsu, K. Okamura, and K. Miya, "Iterative solution technique for 3-D eddy current analysis using T-method," *IEEE Trans. Magn.*, vol. MAG-24, no. 6, pp. 2682–2684, Nov. 1988.
- [5] T. Takagi, M. Hashimoto, S. Arita, S. Norimatsu, T. Sugiura, and K. Miya, "Experimental verification of 3D eddy current analysis code using T-method," *IEEE Trans. Magn.*, vol. 26, no. 2, pp. 474–477, Mar. 1990.
- [6] T. Maceina, P. Bettini, G. Manduchi, and M. Passarotto, "Fast and efficient algorithms for computational electromagnetics on GPU architecture," *IEEE Trans. Nucl. Sci.*, vol. 64, no. 7, pp. 1983–1987, Jul. 2017, doi: [10.1109/TNS.2017.2713888](https://doi.org/10.1109/TNS.2017.2713888).
- [7] E. Tonti, *The Mathematical Structure of Classical and Relativistic Physics: A General Classification Diagram*. Basel, Switzerland: Birkhäuser, 2013.
- [8] L. Codecasa, R. Specogna, and F. Trevisan, "A new set of basis functions for the discrete geometric approach," *J. Comput. Phys.*, vol. 229, no. 19, pp. 7401–7410, 2010.
- [9] L. Gori, *Calcolo Numerico*, 5th ed. Bologna, Italy: Edizioni Kappa, 1999.
- [10] I. D. Mayergoyz and G. Bedrosian, "Iterative solution of 3D eddy current problems," *IEEE Trans. Magn.*, vol. 29, no. 6, pp. 2335–2340, Nov. 1993.